

Gravitating Magnetic Monopole in the Global Monopole Spacetime

J. Spinelly*,

U. de Freitas[†]

and E. R. Bezerra de Mello [‡]

Departamento de Física-CCEN
Universidade Federal da Paraíba
58.059-970, J. Pessoa, PB
C. Postal 5.008
Brazil

March 27, 2022

Abstract

In this paper we study the regular self-gravitating 't Hooft-Polyakov magnetic monopole in a global monopole spacetime. We show that for the large distance, the structure of the manifold corresponds to the Reissner-Nordström spacetime with a solid angle deficit factor. Although we analyze static and spherically symmetric solutions, it is not possible to solve analytically the system of coupled differential equations and only numerical evaluations can provide detailed information about the behavior of this system at the neighborhood of the defect's core. So, for this reason we solve numerically the set of differential equations for the metric tensor and for the matter fields for different values of the Higgs field vacuum expectation value, η , and

*E-mail: spinelly@fisica.ufpb.br

[†]E-mail: umbelino@ccen.ufpb.br

[‡]E-mail: emello@fisica.ufpb.br

the self-coupling constant, λ .

PACS: 04.20-q, 41.20-q, 04.20Jb, 11.15Ex.

1. Introduction

The self-gravitating 't Hooft-Polyakov magnetic monopole [1] in a curved spacetime has been studied a few years ago considering it as a magnetic point charge [2, 3]. The exact solution obtained for the metric tensor has the Reissner-Nordström form corresponding to a point (magnetic) charge $g = 1/e$. A regular solution for this system has been presented by Nieuwenhuizen *et al* [4]. There, they have constructed a positive-definite functional energy function of the matter fields only. They claimed that this is enough to prove the existence of non-singular monopole solutions. More recently Lee *et al* [5] and Ortiz [6] have shown that non-singular monopole solutions exist only if the Higgs vacuum expectation value, η , is smaller or equal to a critical value, η_{cr} , which is of order of the Planck mass. In the limiting case the monopole becomes a black hole, with the region outside the horizon described by the Reissner-Nordström solution.

Barriola and Vilenkin [7] have analyzed the effect in the geometry of the spacetime produced by a system composed by Higgs field only, which undergoes to a spontaneous breakdown of global $O(3)$ gauge symmetry. They noticed that the solution for the metric tensor is similar to the Schwarzschild spacetime with an additional solid angle deficit and a nonzero scalar curvature. They pointed out that for large value of the geometric mass, the model describes a black hole carrying a global monopole.

One of the main differences between the large distance behaviors in the geometries of the spacetime produced by both topological defects, the local and the global monopoles, is due to their energy densities, which for the global monopole case decreases as $1/r^2$. This behavior is responsible for the solid angle deficit presented by this geometry.

In this paper we continue the discussion related with this topic and consider both type of topological defects in the same model. We analyze the effects produced by local and global monopole on the geometry of the manifold. We investigate the possibility of this system to present regular solution and we also analyze its behavior near and far away from the defect's core. So the basic idea of this model is to describe a regular topological defect which presents a magnetic field besides to present a solid angle deficit.

Assuming the existence of such object in a typical galaxy, the total energy contained inside it would be strongly provided by the global Higgs field [8]

¹. Astrophysics bounds on the flux of magnetic monopole and evidence that the galactic magnetic field is mainly azimuthal [9] indicate that the excess number density of such object, if they really exist, is very small. Moreover, upper bounds on the number density of global monopole is at most one in the local group of galaxies as pointed out by Hiscock [10].

Differently from a pure global monopole, this composite topological defect exerts a gravitational interaction on surrounding matter, apart from the electromagnetic one on charged particles. So, such object shares with both, global and magnetic monopole, some of their relevant properties. Numerical simulation related with the upper bound on the number density of them in the Universe, may be developed in a similar manner as it was developed to global monopole only in the paper by Bennett and Rhie [11].

The complete information about this system requires the knowledge of the behaviors of the matter and gravitational fields, i.e., we have to know how these fields change along the distance and how they are connected; besides we also want to know how these fields' behaviors are affected when the energy scale of breakdown of gauge symmetry and the Higgs self-coupling are varying. Because it is impossible to solve analytically the complete set of coupled differential equation associated with this system, only numerical analysis makes possible to obtain these informations. Numerical analysis of self-gravitating magnetic monopole has been developed by several authors, see for example Refs. [5] and [12]. For the global monopole case Harari and Loustó [13] have shown numerically the behavior of the Higgs field and how it is affected by the variation of the parameter η . More recently Maison [14] and Liebling [15] have analyzed the stability condition for the global monopole solution. They found that for η bigger than some critical value, the global monopole fail to be static.

This paper is organized as follows. In section 2 we briefly review some of the relevant characteristics of the local and global monopole in a curved spacetime. We also introduce the model used to describe the system which presents the topological defect formed by both monopoles and derive the equations of motion which governs the behavior of this object. Because it is

¹In fact, the energy density outside the global monopole is $T_t^t \approx -\eta^2/r^2$, consequently the total Newtonian mass inside a space region of radial extent R is $E(R) \approx 4\pi G\eta^2 R$. Considering R the typical radius of a galaxy $R \approx 15Kpc$ and for the symmetry breaking scale $\eta \approx 10^{16}GeV$ which is the value for grand unified theories, this total energy due to the global monopole is approximately ten times the mass of the galaxy.

impossible to solve analytically this set of differential equations we leave for the section 3 its numerical analysis. From our results it is possible to exhibit the behaviors for matter and gravitational fields, their dependence with the distance from the point to the monopole's core and how they are connected among other pertinent informations. In section 4 we present our conclusions and some important remarks about this paper.

2. Field Equation for the Compost Topological Defect

In this section we introduce the model which, by a spontaneous breakdown of gauge symmetry, gives rise to a non-Abelian magnetic and global monopoles in a curved spacetime. This defect presents both properties of its constituent: a magnetic field and a solid angle deficit. Below we shall briefly review both topological defects separately.

The global monopole is a defect obtained by a system composed by a self-coupling Higgs isotriplet field which undergoes to a spontaneous breakdown of global $O(3)$ gauge symmetry to $U(1)$. Coupling this matter field with the Einstein equation, a spherically symmetric metric tensor given by the line element

$$ds^2 = -B(r)dt^2 + A(r)dr^2 + r^2(d\theta^2 + \sin^2\theta d\phi^2) , \quad (1)$$

presents regular solutions for the radial functions $B(r)$ and $A(r)$, that for points far from the monopole's core are given by [7]

$$B(r) = A(r)^{-1} = 1 - 8\pi G\eta^2 - 2GM/r , \quad (2)$$

η being the scale energy where the symmetry is broken. The parameter M is approximately the mass of the monopole. Neglecting the mass term and rescaling the time variable, we can rewrite the monopole metric tensor as

$$ds^2 = -dt^2 + \frac{dr^2}{\alpha^2} + r^2(d\theta^2 + \sin^2\theta d\phi^2) , \quad (3)$$

where the parameter $\alpha^2 = 1 - 8\pi G\eta^2$ is smaller than unity. The above geometry presents no Newtonian potential, it is not flat² and the solid angle of a sphere of unity radius is $4\pi\alpha^2$, so smaller than 4π .

²The scalar curvature associated with this spacetime is $R = \frac{2(1-\alpha^2)}{r^2}$.

The energy-momentum tensor associated with the matter field, outside the monopole's core can be approximately written by

$$T_t^t \approx T_r^r \approx -\frac{\eta^2}{r^2}, \quad T_\theta^\theta \approx T_\phi^\phi \approx 0, \quad (4)$$

consequently the energy is linearly divergent at large distance: $E(r) \approx 4\pi G\eta^2 r$.

The magnetic monopole is also a topological defect described by a system composed by a self-coupling Higgs isotriplet field which interacts with a Yang-Mills gauge field. This system presents a local $SO(3)$ gauge symmetry which is spontaneously broken down to $U(1)$. In a flat spacetime this theory gives rise to 't Hooft-Polyakov monopole with magnetic charge and finite energy [1]. This system has been firstly analyzed in a curved spacetime in Refs. [2, 3]. In these papers the authors have shown that this system presents as an exact solution a metric tensor identical with the Reissner-Nordström one

$$B(r) = \frac{1}{A(r)} = 1 - \frac{2GM}{r} + \frac{4\pi G}{e^2 r^2}, \quad (5)$$

where M is a constant of integration, identified as the mass of the monopole and $1/e$ is its magnetic charge.

The energy-momentum tensor associated with the matter fields compatible with this singular solution is

$$T_t^t = T_r^r = -T_\theta^\theta = -T_\phi^\phi = -\frac{1}{2e^2 r^4}. \quad (6)$$

In their remarkable paper Nieuwenhuizen *et al* [4] have proved the existence of non-singular self-gravitating magnetic monopole. In order to do that, they have constructed a positive-definite functional energy whose minimum value was claimed to be attained by a stable non-singular solution. They also have presented the boundary conditions obeyed by regular solutions at the monopole's core and show that the asymptotic form of the metric tensor is a Reissner-Nordström geometry. More recently Lee *et al* [5] and Ortiz [6] have analyzed again the self-gravitating magnetic monopole system and observed that for very heavy monopole there is no non-singular solutions. They pointed out that when $G\eta^2$ becomes large $A^{-1}(r)$ presents a local minimum which approaches to zero; so for some critical value there appears a horizon

and the monopole becomes a black-hole with the region outside to the horizon described by the Reissner-Nordström metric spacetime. They present numerical solutions for the matter and gravitational fields for different values of the parameter η^2 , where explicitly the horizon shows up.

After this brief review let us introduce the model proposed by us. The basic idea of this model is to describe both topological defects on the same time. In order to do that we endow this model with a gauge group product of two different gauge groups symmetry. Because we want to obtain magnetic monopole configuration we have to gauge one of them. Also we introduce two Higgs fields in $(\mathbf{3}, \mathbf{1})$ and $(\mathbf{1}, \mathbf{3})$ representations of the $G := SO_L(3) \otimes O_G(3)$ groups, where the subindices refer to local (L) and global (G) gauge symmetries. The Higgs fields are responsible for the spontaneous break of gauge symmetries $SO_L(3) \otimes O_G(3)$ to $U_L(1) \otimes U_G(1)$. Moreover in order to simplify our analysis we shall consider two situations: The first case is obtained taking the Higgs self-coupling constants and vacuum expectation values the same in both sectors and do not admit a direct coupling between them. The second case is a particular situation of the first one taking the self-coupling associated with the local sector vanishing. In the latter, the system also presents localized self-gravitating magnetic monopole. The Lagrangian density which governs the more general case, i.e., the first one, is:

$$\mathcal{L}_M = -\frac{1}{4}(F_{\mu\nu}^a)^2 - \frac{1}{2}g^{\mu\nu}(D_\mu\phi^a)(D_\nu\phi^a) - \frac{1}{2}g^{\mu\nu}(\partial_\mu\chi^a)(\partial_\nu\chi^a) - V(\phi^a, \chi^a), \quad (7)$$

with the Latin indices referring to the internal gauge groups $a, b = 1, 2, 3$. We also have

$$D_\mu\phi^a = \partial_\mu\phi^a - e\epsilon_{abc}A_\mu^b\phi^c, \quad (8)$$

$$F_{\mu\nu}^a = \partial_\mu A_\nu^a - \partial_\nu A_\mu^a - e\epsilon_{abc}A_\mu^b A_\nu^c, \quad (9)$$

and

$$V(\phi^a, \chi^a) = \frac{\lambda}{4}(\phi^a\phi^a - \eta^2)^2 + \frac{\lambda}{4}(\chi^a\chi^a - \eta^2)^2. \quad (10)$$

In the following analysis we shall consider only static spherically symmetric solutions, for this reason the metric tensor is written in the form presented by (1).

The ansatz adopted to describe both topological defects is the usual one in flat spacetime written in terms of 'Cartesian' coordinates as

$$\chi^a(x) = \eta f(r)\hat{x}^a, \quad (11)$$

$$\phi^a(x) = \eta h(r) \hat{x}^a , \quad (12)$$

$$A_i^a(x) = \epsilon_{iaj} \hat{x}^j \frac{1 - u(r)}{er} , \quad (13)$$

and

$$A_0^a(x) = 0 . \quad (14)$$

Because we are seeking static solutions all properties of the system may be described by the Lagrangian which is the sum of the Einstein one, L_E , and the covariant matter Lagrangian, L_M :

$$L_E = \frac{1}{16\pi G} \int d^3x \sqrt{-g} R \quad (15)$$

and

$$L_M = \int d^3x \sqrt{-g} \mathcal{L}_M . \quad (16)$$

Substituting the configurations (11) - (14) into (7), together with the spherically symmetric metric tensor (1), we obtain for the matter field the following Lagrangian:

$$L_M = -4\pi \int_0^\infty dr r^2 \sqrt{AB} \left[\frac{\mathcal{K}(f, h, u)}{A} + \mathcal{U}(f, h, u) \right] , \quad (17)$$

where

$$\mathcal{K}(f, h, u) = \frac{1}{2}\eta^2(f')^2 + \frac{1}{2}\eta^2(h')^2 + \frac{(u')^2}{e^2 r^2} , \quad (18)$$

and

$$\mathcal{U}(f, h, u) = \frac{(u^2 - 1)^2}{2e^2 r^4} + \frac{\eta^2 u^2 h^2}{r^2} + \frac{\eta^2 f^2}{r^2} + \frac{\lambda \eta^4}{4} (h^2 - 1)^2 + \frac{\lambda \eta^4}{4} (f^2 - 1)^2 , \quad (19)$$

where the primes denote differentiation with respect to r .

The Einstein Lagrangian for the metric tensor (1) reads

$$L_E = \frac{1}{4G} \int_0^\infty dr \left[-\frac{1}{\sqrt{AB}} (r^2 B')' + \frac{r^2 B' A'}{2A\sqrt{AB}} + \frac{r^2 (B')^2}{2B\sqrt{AB}} + \frac{2r A'}{A} \sqrt{\frac{B}{A}} + 2\sqrt{AB} \left(1 - \frac{1}{A}\right) \right] . \quad (20)$$

Following the procedure adopted in [4] it is possible to work with the Lagrangian below, L'_E , which differs from the previous one by a total derivative:

$$L'_E = \frac{1}{4G} \int_0^\infty dr r \sqrt{AB} \left(\frac{1}{A} - 1 \right) \left(\frac{A'}{A} + \frac{B'}{B} \right) . \quad (21)$$

The total Lagrangian for this system can be given as the sum of (17) with (21). As we can see (21) can be written in terms of two new radial fields $X = \sqrt{AB}$ and $Y = \sqrt{B/A}$. The Euler-Lagrange equations for the gravitational degrees of freedom can be obtained by:

$$(rY)' = X (1 - 8\pi Gr^2 \mathcal{U}) \quad (22)$$

and

$$\frac{X'}{X} = 8\pi Gr \mathcal{K} . \quad (23)$$

Integrating (23) assuming that at infinity $X(\infty) = 1$ we obtain

$$A(r) = \frac{1}{B(r)} \exp \left[16\pi G \int_0^r dr' r' \mathcal{K}(f, h, u) \right] . \quad (24)$$

Now going back to (22) we obtain

$$\left(\frac{r}{A} \right)' = 1 - 8\pi Gr^2 \left[\frac{\mathcal{K}(f, h, u)}{A} + \mathcal{U}(f, h, u) \right] . \quad (25)$$

Integrating the above equation assuming the regularity condition on $r/A(r)$ at origin, we have

$$\frac{1}{A(r)} = \alpha^2 - \frac{2GM(r)}{r} , \quad (26)$$

being $\alpha^2 = 1 - 8\pi G\eta^2$ and $M(r)$ given by the integral

$$M(r) = 4\pi \int_0^r dr' r'^2 \left[\frac{\eta^2}{2A} [(f')^2 + (h')^2] + \frac{(u')^2}{Ae^2 r'^2} + \frac{\eta^2 u^2 h^2}{r'^2} + \eta^2 \frac{(f^2 - 1)}{r'^2} + \frac{(u^2 - 1)^2}{2e^2 r'^4} + \frac{\lambda \eta^4}{4} (h^2 - 1)^2 + \frac{\lambda \eta^4}{4} (f^2 - 1)^2 \right] . \quad (27)$$

We can also rewrite $M(r)$ in a different way substituting (26) into the right hand side of (25). After some steps we get

$$M(r) = \exp \left[- \int_0^r dr' p(r') \right] \int_0^r dr' q(r') \exp \left[\int_0^{r'} dr'' p(r'') \right] , \quad (28)$$

with

$$p(r) = 8\pi Gr\mathcal{K}(f, h, u) \quad (29)$$

and

$$q(r) = 4\pi \left[r^2 \left(\alpha^2 \mathcal{K}(f, h, u) + \mathcal{U}(f, h, u) \right) - \eta^2 \right] . \quad (30)$$

With this procedure we have removed the factor $1/A(r)$ in the integral definition of $M(r)$ given in (27). From the above equations we can obtain the total mass written as

$$\mathcal{M} = M(\infty) = 4\pi \int_0^\infty \left[r^2 \left(\mathcal{U}(f, h, u) + \alpha^2 \mathcal{K}(f, h, u) \right) - \eta^2 \right] e^{-P(r)} , \quad (31)$$

where

$$P(r) = 8\pi G \int_r^\infty dr' r' \mathcal{K}(f, h, u) , \quad (32)$$

which is a positive-definite quantity.

The gravitational field equations, (22) and (23) can be rewritten in a different way in terms of the radial function $M(r)$ as follows:

$$\frac{(AB)'}{AB} = 16\pi Gr\mathcal{K}(f, h, u) \quad (33)$$

and

$$M'(r) + 8\pi Gr\mathcal{K}M(r) = 4\pi r^2 \left(\mathcal{U} + \alpha^2 \mathcal{K} \right) - 4\pi \eta^2 . \quad (34)$$

For the matter fields we have:

$$\frac{1}{\sqrt{AB}} \left[\sqrt{\frac{B}{A}} u' \right]' = \frac{e^2 r^2}{2} \frac{\partial \mathcal{U}}{\partial u} = \frac{u(u^2 - 1)}{r^2} + \eta^2 e^2 h^2 u , \quad (35)$$

$$\frac{1}{r^2 \sqrt{AB}} \left[r^2 \sqrt{\frac{B}{A}} h' \right]' = \frac{1}{\eta^2} \frac{\partial \mathcal{U}}{\partial h} = \frac{2hu^2}{r^2} + \lambda \eta^2 h(h^2 - 1) , \quad (36)$$

and

$$\frac{1}{r^2\sqrt{AB}} \left[r^2 \sqrt{\frac{B}{A}} f' \right]' = \frac{1}{\eta^2} \frac{\partial \mathcal{U}}{\partial f} = \frac{2f}{r^2} + \lambda \eta^2 f(f^2 - 1) . \quad (37)$$

From these set of differential equations it is possible to observe that there is no direct interaction between the global Higgs field expressed in terms of $f(r)$ with the magnetic sector represented by $h(r)$ and $u(r)$. However the gravitational field interacts with both sectors. Moreover these equations are invariant under the discrete symmetries $f \rightarrow -f$, $h \rightarrow -h$ and $u \rightarrow -u$. The first two transformations correspond to specific choice of monopoles configurations and the last one corresponds to a gauge transformation.

In order to analyze this set of differential equations let us first discuss the boundary conditions obeyed by the fields.

The boundary condition on the matter fields at infinity follows by the requirement of the topological defect be localized

$$f \rightarrow \pm 1, \quad h \rightarrow \pm 1 \text{ and } u \rightarrow 0 . \quad (38)$$

Due to the presence of the global Higgs sector, the metric components do not asymptote to unity. So according to the results exhibited for the purely global monopole spacetime we can write the following boundary conditions at infinity:

$$AB \rightarrow 1 \text{ and } M/r \rightarrow 0 . \quad (39)$$

The last two conditions above follows from the previous one obeyed by the matter fields, as can be easily observed by the expressions (18) and (19). The double sign which appear for the behavior of h and f at infinity corresponds to the monopole or anti-monopole configurations. In this paper we shall adopt the positive sign for both Higgs fields.

The boundary conditions at origin required by regularity of our solutions are:

$$u \rightarrow 1, \quad f \rightarrow 0, \quad h \rightarrow 0, \quad AB \rightarrow 1, \text{ and } M \rightarrow -4\pi\eta^2 r . \quad (40)$$

Being satisfied these conditions, the behavior of the integrand for the Lagrangian associated with the matter and gravitational fields, Eqs. (17) and (21), vanish at origin.

As it was pointed out in Refs. [2, 3], the differential equations obeyed by the matter fields associated with the local monopole sector only, admit exact

(singular) solution $u = 0$ and $h = 1$ everywhere. However as to the global monopole sector, the field f goes to unity only at infinity.

So, unfortunately the complete set of differential equations does not admit closed solution, even singular one. So the relevant aspects about this compost defect can only be observed numerically. We leave this analysis for the next section. Before to end the present section we would like to make two comments about this model:

a) The first one refers to the positive-definite functional energy property enjoyed by this model. In fact, eliminating the gravitational degrees of freedom from the total Lagrangian, $L_T = L_M + L'_E$, by using (23), we obtain an energy-functional, $E = -L_T$, expressed in terms of the matter fields as:

$$E = \int d^3x \sqrt{-g} (\mathcal{U} + \mathcal{K}) . \quad (41)$$

b) The second point that we want to mention is that a pointlike topological defect which takes into account a (point) magnetic charge $g = 1/e$ in a solid angle deficit geometry, can be obtained by considering a non-dynamical energy-momentum tensor below in the Einstein equation:

$$T_t^t = T_r^r = -\frac{1}{r^2} \left(\frac{1}{2e^2 r^2} + \eta^2 \right), \quad T_\theta^\theta = T_\phi^\phi = \frac{1}{2e^2 r^4} . \quad (42)$$

The gravitational field associated with the above tensor reads:

$$B(r) = \frac{1}{A(r)} = \alpha^2 - \frac{2GM}{r} + \frac{4\pi G}{e^2 r^2} , \quad (43)$$

which corresponds to the Reissner-Nordström spacetime with an additional solid angle deficit factor. This metric tensor, as mentioned above, describes the effect produced in the geometry by two distinct objects: the global monopole, responsible for a solid angle deficit, and the magnetic monopoles, responsible for a non-vanishing radial magnetic field

$$B_i = B_i^a \hat{\phi}^a = \hat{x}_i / er^2 . \quad (44)$$

Although the above expressions represent exact solutions for this system, unfortunately they cannot be accepted as physical solution. The non-integrable factor $1/r^4$ of T_t^t provides an infinity energy inside a finite space region around the defect. Finally we want to say that the scalar curvature associated with the above spacetime is $R = \frac{2(1-\alpha^2)}{r^2}$.

3. Numerical Analysis

In this section we shall exhibit the most relevant aspects about this compost defect under a numerical analysis. Our strategy is to present numerical solutions for the matter and gravitational fields which obey regularity conditions at origin. See Eq. (40). Mainly we are interested to analyse their behaviors as the parameters η , associated with the energy scale where the symmetry is spontaneously broken and λ , the self-coupling constant, both vary. In order to start the numerical analysis we shall express the set of differential equations, (33) - (37), in terms of two dimensionless parameters $\Delta = 8\pi G\eta^2$ and $\beta = \lambda/e^2$, rescaling the radial coordinate r as $x = r\eta$.

The case $\Delta = 0$, i.e., $G = 0$ corresponds to the flat-space one. The solutions for the matter fields is the 't Hooft-Polyakov magnetic monopole for the local sector with the global sector independent. Choosing $\beta = 0$ the solution for the u and h can be given in a closed form [16]. As to the global sector, vanishing β the system does not provide localized solution: the differential equation for f becomes linear and a regular solution at origin diverges as $r \rightarrow \infty$. An intermediate situation happens when we assume $\Delta \neq 0$ and the self-coupling constant for the local Higgs sector only vanishes. In this case the matter field equation becomes

$$\frac{1}{\sqrt{AB}} \left(\sqrt{\frac{B}{A}} u' \right)' = \frac{u(u^2 - 1)}{x^2} + h^2 u, \quad (45)$$

$$\frac{1}{x^2 \sqrt{AB}} \left(x^2 \sqrt{\frac{B}{A}} h' \right)' = \frac{2hu^2}{x^2} \quad (46)$$

and

$$\frac{1}{x^2 \sqrt{AB}} \left(x^2 \sqrt{\frac{B}{A}} f' \right)' = \frac{2f}{x^2} + \beta f(f^2 - 1), \quad (47)$$

where the primes in the above equations denote differentiation with respect to x .

As we have said before, in this section we shall analyse, numerically, both cases: The first one described by Eqs. (33) - (37), and the second one by Eqs. (45) - (47).

Now let us start first with the complete model. Casting the differential equations in first-order form by auxiliaries fields $P = u'$, $Q = h'$, $D = f'$

and defining a new other variable $g = 1/A$, the set of differential equations becomes

$$P = u', \quad Q = h', \quad D = f', \quad g = 1/A, \quad (48)$$

$$g' = \frac{1}{x} - \frac{g}{x} - \Delta x \left[U(f, h, u) + g \left(\frac{P^2}{x^2} + \frac{Q^2}{2} + \frac{D^2}{2} \right) \right], \quad (49)$$

$$P' = \frac{1}{g} \left[\frac{gP}{x} - \frac{P}{x} + \frac{u(u^2 - 1)}{x^2} + h^2 u + \Delta x P U(f, h, u) \right], \quad (50)$$

$$Q' = \frac{1}{g} \left[\frac{2hu^2}{x^2} + \beta h(h^2 - 1) - \frac{gQ}{x} - \frac{Q}{x} + \Delta x Q U(f, h, u) \right] \quad (51)$$

and

$$D' = \frac{1}{g} \left[\frac{2f}{x^2} + \beta f(f^2 - 1) - \frac{gD}{x} - \frac{D}{x} + \Delta x D U(f, h, u) \right], \quad (52)$$

being

$$U(f, h, u) = \frac{(u^2 - 1)^2}{2x^4} + \frac{u^2 f^2}{x^2} + \frac{f^2}{x^2} + \frac{\beta}{4}(h^2 - 1)^2 + \frac{\beta}{4}(f^2 - 1)^2. \quad (53)$$

Near the origin, regular solutions must behave as

$$f = c_f x + O(x^3), \quad h = c_h x + O(x^3), \quad u = 1 - c_u x^2 + O(x^4), \quad (54)$$

and

$$g = 1 - \Delta \left[2c_u + \frac{1}{2}(c_f^2 + c_h^2) + \frac{\beta}{6} \right] x^2 + O(x^4), \quad (55)$$

where the three constants c_f , c_h and c_u must be chosen in order to have f , h and u approaching to the correct values as $x \rightarrow \infty$.

The case $c_h = c_u = 0$ and $c_f \neq 0$ corresponds to the global monopole spacetime. In this case there is only one constant to be adjusted. The set of differential equations presents only one parameter Δ . This model has been first numerically analyzed by Harari and Loustó [13]. There, they show that the behavior of the Higgs field is quite insensitive to the values of Δ in the interval $0 \leq \Delta \leq 1$. More recently, Maison and Liebling [14] and Liebling [15] returned to the numerical analysis of this model and found that for $\Delta \geq 1$, $1/A$ decreases toward zero indicating the presence of a horizon.

A more complicated case is when $c_f = 0$ with c_h and c_u different from zero. This case corresponds to a gravitating magnetic monopole. There

are two constants to be adjusted numerically in order the system to present localized topological defect. This model has been analyzed by Lee *et al* [5], Ortiz [6] and Breitenlohner *et al* [12]. In these papers the authors observed that the system presents singular solutions when Δ is greater than some critical value, Δ_{cr} . For these situations $1/A$ has zeros, the Schwarzschild radius becomes greater than the monopole's size, so the monopole must be a black-hole.

Now returning to our system, we present in what follows our numerical results. Defining by the radius of the global and magnetic monopoles' core the value of the dimensionless variable x corresponding to $f(x_L) = 0.9$ and $h(x_G) = 0.9$, respectively, we can observe by Figs. 1(a) and 1(b), that $r_L < r_G$. Also we can notice that both radiuses decrease as β becomes larger. So, these results confirm that, for this model, the magnetic monopole configuration approaches to its vacuum value faster than the global monopole. In this sense the magnetic monopole's core is firstly formed. Moreover, other graphs not included in this paper indicate that the shapes of $f(x)$ and $h(x)$ are almost insensitive to the values of the parameter Δ .³

The Figs. 2(a) and 2(b) display the behavior of the function $u(x)$ with x for different values of β and Δ . From them it is possible to observe that its behavior is sensitive to the values of the parameters Δ and β , in such way that u reaches its asymptotic value faster for greater values of these two parameters.

The Figs. 3(a) and 3(b) exhibit the behavior of the fields f and h for fixed value of Δ and different values of β . We can see that their behaviors are very sensitive to this parameter, and that their radius decrease when β increases. From numerical point of view, solutions with large β become more difficult to be analysed, this is the reason why they are presented in different intervals of the variable x .⁴

As to $g(x) = \frac{1}{A(x)}$, which asymptotes to non-unity values $\alpha^2 = 1 - \Delta$, it develops a local minimum for large values of the parameters Δ and β , independently. Moreover, as Δ increases the asymptotic value of g decreases toward zero, and becomes negative for $\Delta > 1$ indicating the presence of a horizon. So, for $\Delta \geq 1$ this system presents a horizon for any nonzero value

³A similar conclusion has been reached by Harari and Loustó [13] in their analysis of a pure global monopole system

⁴The stability problem related with numerical solutions for large β has been pointed by Breitenlohner *at all* in Ref. [12] for $\beta > 5$ in the gravitating magnetic monopole system.

of β . However, for $\Delta < 1$ there exist a critical value for β above which this compost defect becomes a black hole. To find a domain of existence of regular solution is possible only formally, analysing the set of differential equations at horizon, i. e., substituting $g = 0$ at the point $x = x_H$ in the set. Only numerical calculations allows the obtainement of related parameters β and Δ associated with a specific singular solution.

The figures 4(a) and 4(b) exhibit the behavior of $M(x)$ with x , being $M(x)$ a dimensionless function obtained by $M(r)$ given in (27). In fact this dimensionless mass function which depends only the two parameter β and Δ is defined by $M(r) = 4\pi\eta/eM(x)$. The asymptotic behavior of $M(x)$ provides information about the effective monopole mass. Fig 4(a) shows that for $\beta = 1$ this function asymptotes a negative value. This very peculiar feature has been detected for the global monopole defect by Harari and Loustó in [13].⁵ However for $\beta = 10$ the Fig. 4(b) shows that the effective mass of this topological defect becomes positive. (The same behavior is observed for $\beta = 80$.) So this compost defect presents repulsive or attractive gravitational interactions which depends on the magnitude of the self-coupling constant λ .

The second case can be numerically analyzed in similar way as the previous one; however some changes must be done in order to take into account the vanishing of the self-coupling constant in the local sector of the system. The first-order differential equation set for this case can be written discarding the terms $h(h^2 - 1)$ in (51) and (53). The behavior for the fields f , h and u at the origin are similar to (54); however for g it is

$$g = 1 - \Delta \left[2c_u + \frac{1}{2} (c_f^2 + c_h^2) + \frac{\beta}{12} \right] x^2 + O(x^4) . \quad (56)$$

Once more three new constants must be chosen in order to have solutions with appropriated behavior at infinity.

The most important characteristic observed by us about this model are summarized below:

i) The Figs. 5(a) and 5(b) show the behavior of the fields f and h . Considering again the same definition to the radius of the defects as given before, we can see that for this case $r_G < r_L$. This is in contrast with the result found in the previous model. So comparing the results found in these two models it

⁵In [13] it was observed that the shape of the curves are very insensitive to Δ in the interval $0 \leq \Delta \leq 1$.

is possible to conclude that the sizes of the global and magnetic monopole's core depends on the intensity of their respective self-interactions. Moreover, we can infer that for specific values of these constants, both topological defects present equal radius, though we cannot ensure that both fields f and h have the same behavior.

ii) The Figs. 6(a) and 6(b) exhibit, respectively, an explicit dependence of u and h with β . Although there is no direct interaction between the local sector, represented by these fields, with the self-coupling constant associated with the global sector, our numerical analysis indicate a sensitive dependence of both fields with λ .

iii) The Fig. 6(c) exhibits the behavior of f with β . In this case its dependence is more prominent than for h , i.e., the radius of the global monopole decreases more rapidly with the increasing of β than the magnetic's one.

As to the effective mass associated with this case, $M(x)$, it is observed the same behavior exhibited in the previous case. So we decided do not included extra figures in this part.

4. Concluding Remarks

In this paper we have presented a model which describes two topological defects at the same time: The global and magnetic monopole in a curved spacetime. The Lagrangian density which governs this system contains two distinct bosonic sectors. In order to make our analysis easier we decided do not include a direct interaction between them. Two different situations were analyzed: the first one considering the Higgs self-interactions and vacuum expectation values equal for both sectors. The second situation is a particular case when we switch off the self-coupling constant associated with the local sector only. In both cases the set of coupled differential equations does not allow to obtain a closed solutions, even singular. Only asymptotic behavior for matter and gravitational fields can be provided analytically. Specifically, for regions very far from the topological defect's core, the spacetime corresponds to a Reissner-Nordström spacetime with a solid angle deficit factor

$$B(r) = \frac{1}{A(r)} = \alpha^2 - \frac{2GM}{r} + \frac{4\pi G}{e^2 r^2} .$$

Here we have provided numerical informations about the behavior of these

fields in a non-asymptotic region. These informations concern to the relative sizes of both defects, their dependence on the two parameters presented in this model, the self-coupling constant, through β , and the gravitational constant, through Δ , etc.

The numerical method applied by us in this paper was double-precision fourth-order Runge-Kutta routine. For all calculations the errors found were of order 10^{-3} or less.

It is our intention to continue investigating the behavior of the fields for larger value of the parameter Δ . As shown in previous papers analysing global [14, 15] and gravitational [5, 4, 12] monopoles, for Δ bigger than some critical value, the system presents horizons. For both distinct cases, the horizons appears when Δ is of order unity.

References

- [1] G. 't Hooft, Nucl. Phys. **B79**, 276 (1974) and A. M. Polyakov, Pisma v. Zh. E.T.F. **20**, 430 (1974), (JETP Lett. **20**, 194 (1974)).
- [2] F. A. Bais and R. J. Russel, Phys. Rev. D **11**, 2692 (1975).
- [3] Y. M. Cho and P. G. O. Freund, Phys. Rev. D **12**, 1588 (1975).
- [4] P. van Nieuwenhuizen, D. Wilkinson and M. J. Perry, Phys. Rev. D **13**, 778 (1976).
- [5] K. Lee, V. P. Nair and E. Weinberg, Phys. Rev. D **45**, 2751 (1992).
- [6] M. E. Ortiz, Phys. Rev. D **45** R2586 (1992).
- [7] M. Barriola and A. Vilenkin, Phys. Rev. Lett. **63**, 341 (1989).
- [8] U. Nucamendi, M Salgado and D. Sudarsky, Phys. Rev. Lett. **84**, 3037 (2000).
- [9] M. S. Turner, E. N. Parker and T. J. Bogdan, Phys. Rev. D **26**, 1296 (1982).
- [10] W. Hiscock, Phys. Rev. Lett. **64**, 344 (1990).
- [11] D. P. Bennett and S. H. Rhie, Phys. Rev. Lett. **65**, 1709 (1990).
- [12] P. Breitenlohner, P. Forgács and D. Maison, Nucl. Phys. **B383**, 357 (1992) and P. Breitenlohner, P. Forgács and D. Maison, Nucl. Phys. **B442**, 126 (1995).
- [13] D. Harari and C. Loustó, Phys. Rev. D **42**, 2626 (1990).
- [14] D. Maison and S. Liebling, Phys. Rev. Lett. **83**, 5218 (1999).
- [15] S. L. Liebling, Phys. Rev. D **61**, 024030 (2000).
- [16] M. K. Prasad and C. M. Sommerfeld, Phys. Rev. Lett. **35**, 760 (1975).

5. Figure Captions

Figure 1: These graphs show simultaneously the behavior of f and h for: (a) $\beta = 1$ and $\Delta = 0.1$ and (b) for $\beta = 80$ and $\Delta = 10^{-6}$.

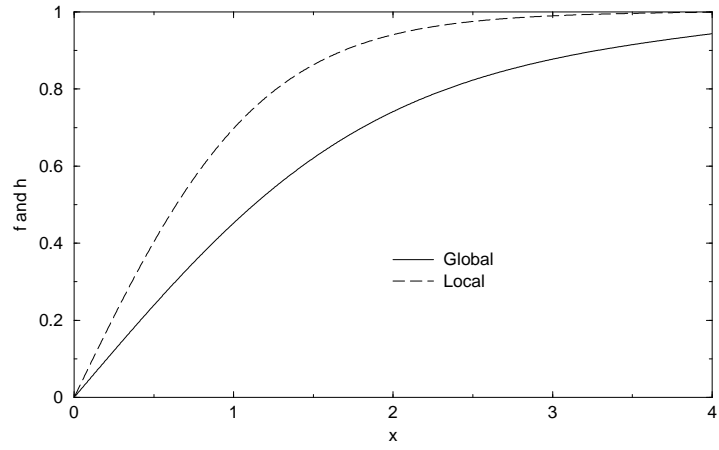
Figure 2: These graphs show the behavior of u for three different values of Δ for (a) $\beta = 10$ and (b) $\beta = 80$.

Figure 3: These graphs show the behavior of (a) f and (b) h for $\Delta = 0.1$ and three different values of β .

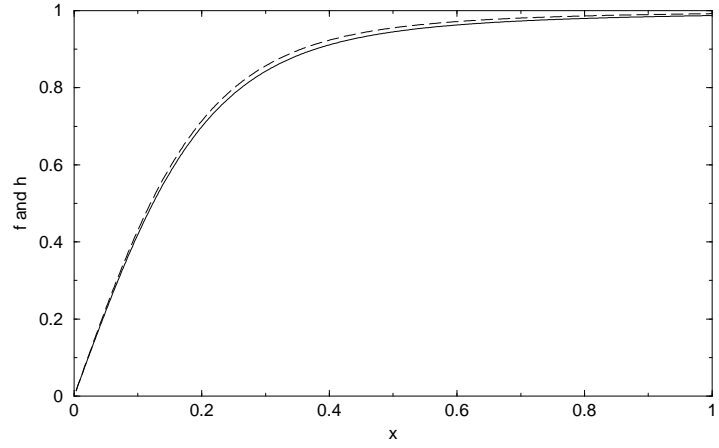
Figure 4: These graphs show the behavior of the effective mass, $M(x)$ for (a) $\beta = 1$ and (b) $\beta = 10$ for three different values of Δ .

Figure 5: These graphs show simultaneously the behavior of f and h for: (a) $\beta = 10$ and $\Delta = 10^{-6}$ and (b) for $\beta = 10$ and $\Delta = 0.1$.

Figure 6: These graphs show the behavior of (a) u , (b) h and (c) f for three different values of β for $\Delta = 0.1$.

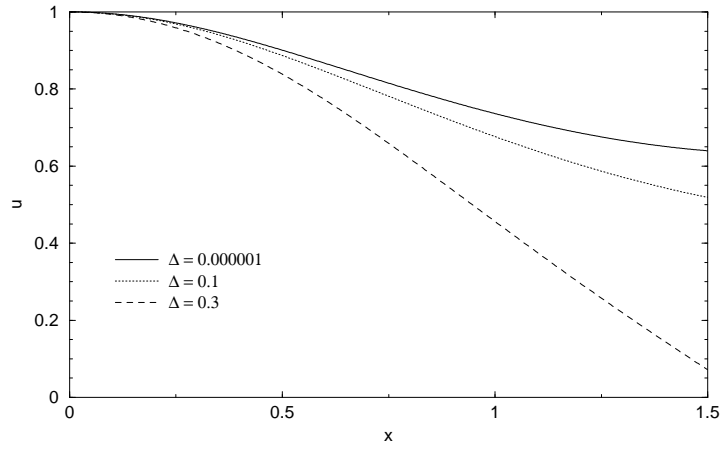


(a)

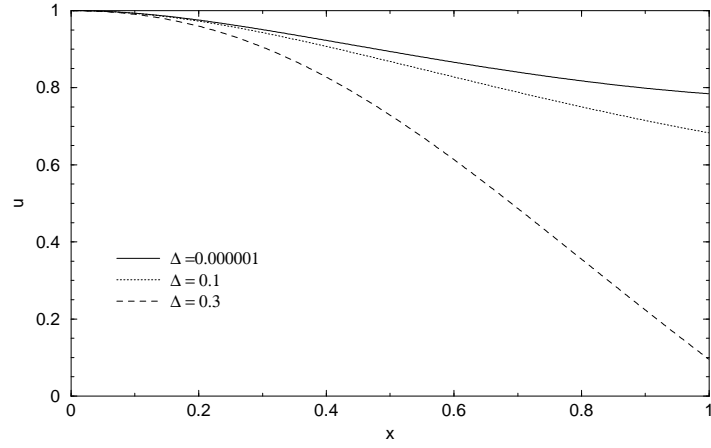


(b)

Figure 1:

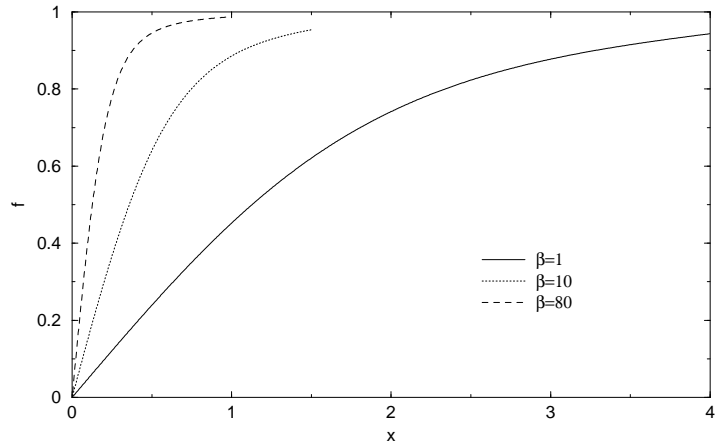


(a)

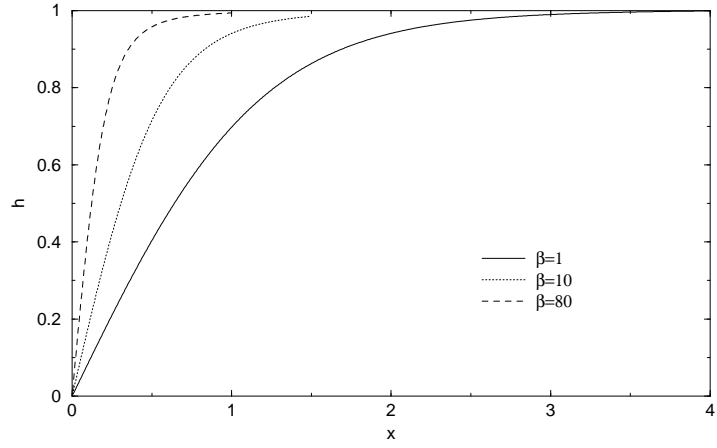


(b)

Figure 2:

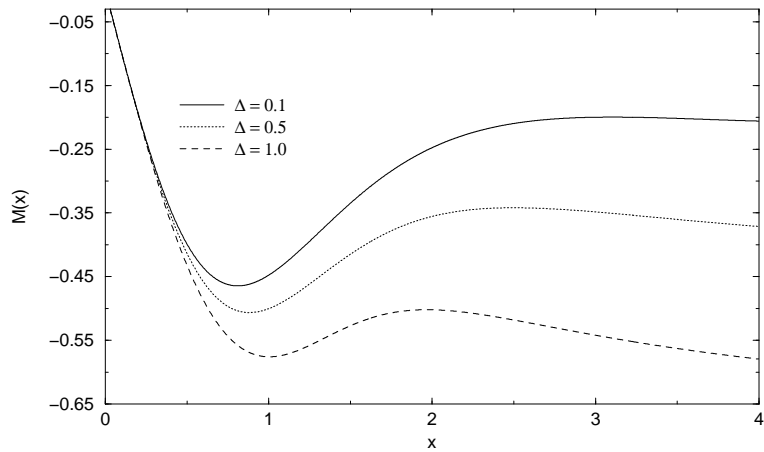


(a)

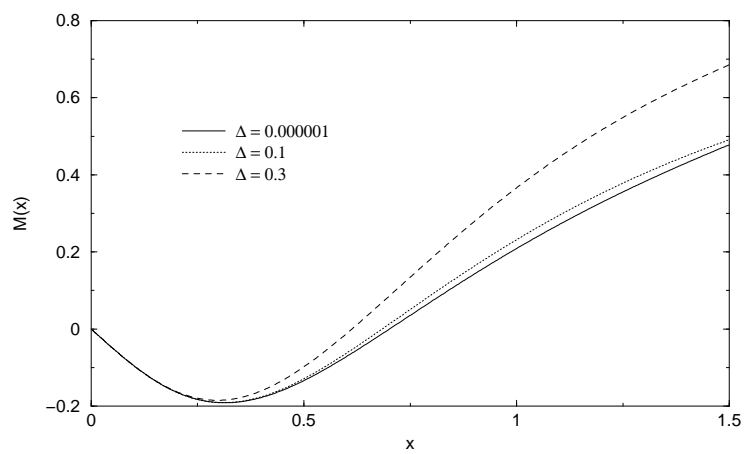


(b)

Figure 3:

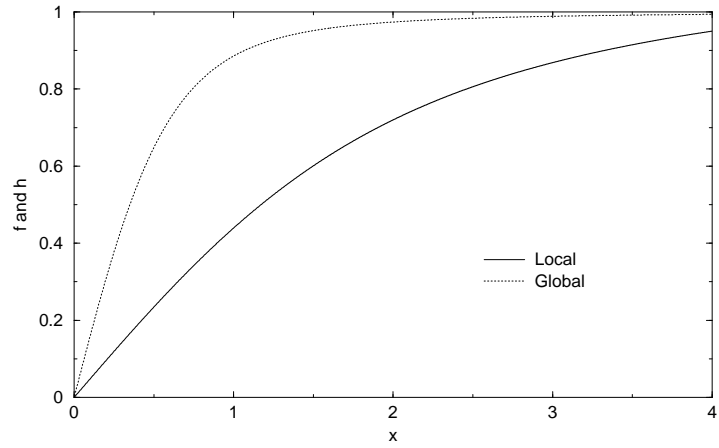


(a)

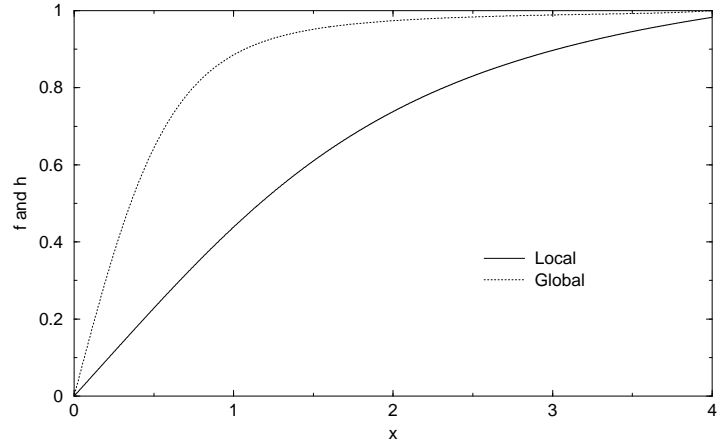


(b)

Figure 4:

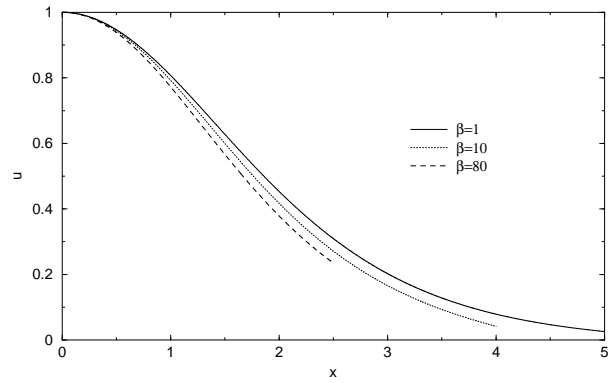


(a)

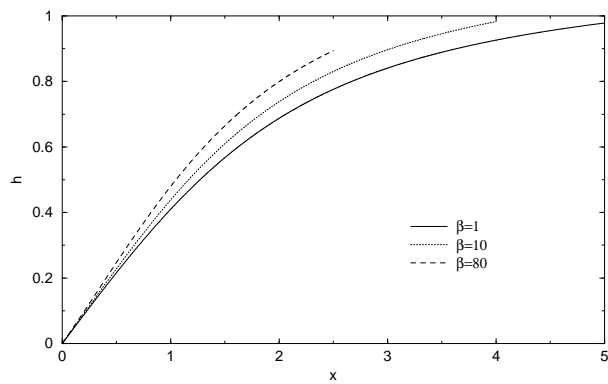


(b)

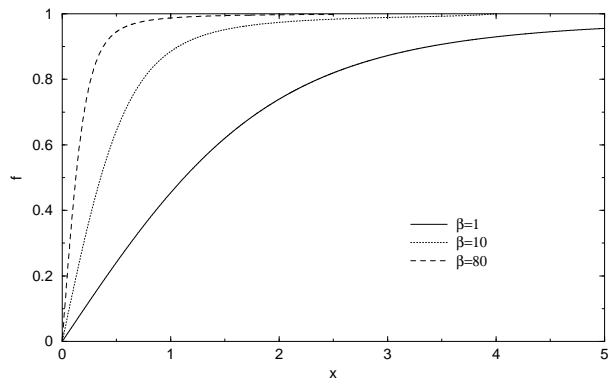
Figure 5:



(a)



(b)



(c)

Figure 6: